

Document downloaded from:

<http://hdl.handle.net/10251/67192>

This paper must be cited as:

Sadykova, SP.; Ebeling, W.; Tkachenko Gorski, IM. (2011). Static and dynamic structure factors with account of the ion structure for high-temperature alkali and alkaline earth plasmas. *European Physical Journal D*. 61(1):117-130. doi:10.1140/epjd/e2010-10118-y.



The final publication is available at

<http://dx.doi.org/10.1140/epjd/e2010-10118-y>

Copyright EDP Sciences

Additional Information

Static and Dynamic Structure Factors with Account of the Ion Structure for High-temperature Alkali and Earth-alkali Plasmas

S. P. Sadykova^{1a}, W. Ebeling^{1b} and I. M. Tkachenko^{2c}

¹ Institut für Physik, Humboldt Universität zu Berlin, Newtonstr. 15, 12489 Berlin, Germany

² Department of Applied Mathematics, Polytechnic University of Valencia, 46022 Valencia, Spain

Received: date / Revised version: date

Abstract. The $e-e$, $e-i$, $i-i$ and charge-charge static structure factors have been calculated for Alkali and Be^{2+} plasmas using Gregori's method [14]. The dynamic structure factors for Alkali plasmas have been calculated using Adamjans' et al method [52], [53]. In both methods the screened Hellmann-Gurskii-Krasko potential, obtained on a base of Bogoljubow method, has been used taking into account not only the quantum-mechanical effects but also the ion structure [13].

PACS. 52.38.Ph X-ray scattering – 52.27.Aj Alkali and Earth-alkali Plasmas

1 Introduction

The structure and thermodynamic properties of Alkali and earth-alkali plasmas are of basic interest and of importance for high-temperature technical applications. In the environment of the critical point the materials are in the thermodynamic state of a strongly coupled plasma. Here we will go far beyond the critical point to the region of nearly fully ionised plasmas which is $T \geq 30000K$ for Alkali and $T \geq 100000K$ for earth-alkali plasmas. The

investigation of thermodynamic properties in Alkali plasmas under extreme conditions is not only important for basic research. There are many applications, e.g. in material sciences, geophysics and astrophysics. Furthermore, these studies throw light on the complex picture of phase transitions in metal vapors which play an outstanding role in technology.

Over the past years a considerable amount of effort has been concentrated on the experimental [1]-[5] and theoretical [6]-[9] investigation of the behavior of Alkali metals in the liquid and plasma state expanded by heating toward

^a *e-mail:* saltanat@physik.hu-berlin.de

^b *e-mail:* ebeling@physik.hu-berlin.de

^c *e-mail:* imtk @ mat.upv.es

Table 1. The ionization energies I_i (eV) of Alkali and Be atoms

	H	Li	Na	K	Rb	Cs	Be
I_1	13.595	5.39	5.138	4.339	4.176	3.893	9.306
I_2	-	75.62	47.29	31.81	27.5	25.1	18.187

the liquid-vapor critical point. High-temperatures Alkali plasmas are widely applied in many technical projects. For instance, Li is an Alkali metal of considerable technological interest. Lithium is planned to be used in inertial confinement fusion, solar power plants, electrochemical energy storage, magnetohydrodynamic power generators and in a lot of further applications. Recent advances in the field of extreme ultraviolet EUV lithography have revealed that laser-produced *Li* plasmas are source candidates for next-generation microelectronics [11], [12]. For this reason we believe that the study of basic properties of Alkali plasmas, like the microfield distributions are of interest. In the previous work we studied Li^+ plasma [13]. In this work, we consider Li^+ , Na^+ , K^+ , Rb^+ , Cs^+ and Be^{2+} plasmas. For simplicity of the calculations we take into account here only single ionization for Alkali plasmas ($n_e = n_i$) and doubled for Beryllium plasma ($n_e = 2n_i$), where n_e , n_i are the concentrations of electrons and ions respectively. Li, Na, K, Rb, Cs atoms have one outer electron and Be^{2+} has two outer electrons. In the table 1 the ionization energies of Alkali atoms and Berillium atom are presented. Correspondingly we will study temperatures around $30000K$ and $100000K$, where most of outer electrons are ionized, but the rest core electrons are still

tightly bound.

Recently, X-ray scattering has proved as a powerful technique in measuring densities, temperatures and charge states of warm dense matter regimes. In inertial confinement fusion and laboratory astrophysics experiments the system experiences a variety of plasma regimes and of high interest are the highly coupled plasmas $\Gamma_{ii} \geq 1$, $\Gamma_{ii} = z^2 e^2 / (4\epsilon_0 k_B T r_{ii})$ with $r_{ii} = (3/4\pi n_i)^{1/3}$ and the electron subsystem exhibiting partial degeneracy. Such regimes can be often found during plasma-to-solid phase transitions. Recent experiments with a solid density Be plasma have shown high ion-ion coupling regimes and their interpretation must account for significant strong coupling effects. The present study is devoted to the study the of the static and dynamic structure factors for Alkali and Be^{2+} plasmas at temperatures $T \geq 30000K$ and $T \geq 100000K$. The structure factors are the fundamental quantity that describes the X-ray scattering cross-section from a plasma. Since they are related to the density fluctuations in the plasma, they directly enter into the expressions for the total cross-section. In the case of a weakly coupled plasma SF can be obtained from the Debye-Hückel theory or the random phase approximation (RPA), while at moderate coupling the RPA fails to predict the correct spatial correlations. However, recent work (Gregori et al, Arkhipov et al.) has shown that the technique developed in the classical work of Bogoljubov provides good expresses of SF for moderately coupled plasmas.

For determination of the static and dynamic structure factors one needs to have a screened pseudopotential as

an essential input value. The semiclassical methods allow to include the quantum-mechanical effects by appropriate pseudopotentials which resolve divergency problem of the electric fields at small distances. This method was pioneered by Kelbg, Dunn, Broyles, Deutsch and others [20] - [24] and later significantly improved [25],[26]. These models are valid for highly temperature plasmas when the ions are bare or there is no significant influence of the ion shell structure. In order to correctly describe Alkali plasmas at moderate temperatures one needs to take into account the ion structure. For example, for the behaviour of Alkali plasmas the short range forces between the charged particles are of great importance. For Alkali plasmas at small distances between the particles deviations from Coulomb law are observed which are mainly due to the influence of the core electrons. The method of model pseudopotentials describing the ion structure was pioneered by Hellmann. Hellmann demonstrated, using the Thomas-Fermi model, that the Pauli exclusion principle for the valence electrons can be replaced by a non-classical repulsive potential [27]. This method was later rediscovered and further developed for metals by Heine, Abarenkov and Animalu [28]-[30]. Heine, Abarenkov proposed a model, where one considers two types of interaction: outside of the shell, where the interaction potential is Coulomb and inside, where it is the constant. Parameters of this model potentials were determined using the spectroscopic data. Later on the different pseudopotential models were proposed. For the more detailed review we refer a reader to [30]. All these models have the one

disadvantage. Their Fourier transforms (formfactor) are not sufficiently convergent when the Fourier space coordinate goes to infinity. Gurskii and Krasko [31] proposed a model potential which eliminates this problem and provides smoothness of the pseudopotential inside the shell giving its finite value at small distances. First attempt to construct the model for Alkali plasmas taking into account ion structure was made in works [33]-[35] where the Hellmann type pseudopotentials were used. In this work we use Hellmann-Gurskii-Krasko pseudopotential model for electron-ion interactions and its modified version of ion-ion interactions. There is also a high interest to construct a pseudopotential model of particle interaction in the dense plasma taking into an account not only the quantum-mechanical effects including ion shell structure at short distances but also screening field effects. In the work [13] the screened Hellmann-Gurskii-Krasko potential was derived by using Bogoljubow's method as described e.g. in [36], [37], [38] and [39].

We consider Li^+ , Na^+ , K^+ , Rb^+ , Cs^+ and Be^{2+} plasmas of a TCP with the charges $Ze_- = -e_+$ and masses $m_i \gg m_e$ and the densities $n_e = Zn_i$ ($Z = 1, 2$). We will calculate here the static and dynamic structure factors in TCP, including quantum effects and the ion shell structure using Hellmann-Gurskii-Krasko pseudopotential (HGK) and find the corresponding radial distribution functions. For determination of the static and dynamic structure factors we use the screened Hellmann-Gurskii-Krasko potential obtained in [13]. The method which is used for the calculation of the static structure factor is the Gregori et

al.while for dynamic - the V.M. Adamjan et al. for two-component plasmas [52], [53]. We would like to underline again that the inclusion of both components into the theory and a correct account of the short-range electron-ion interactions, is very essential for an understanding of the structure factors in the plasma.

2 Pseudopotentials taking into account the ion structure. Hellmann-Gurskii-Krasko potential

Clearly, the Coulombic law is not applicable to the forces between the charges in Alkali plasmas since there are strong deviations from Coulombs law at small distances due to the influence of core electrons.

In many problems of atomic and molecular physics one can divide the electrons of the system into valence and core electrons. Often the important physical properties are determined by the valence electrons. In a series of pioneering papers Hellmann attempted to develop a computational model in which the treatment of such atoms and molecules is reduced to the treatment of valence electrons [27]. Hellmann demonstrated that the Pauli exclusion principle for the valence electrons can be replaced by a nonclassical potential (*Abstossungspotential*) which is now called the *pseudopotential*. Hellmann's idea was to replace the requirement of orthogonality of valence orbital to the core orbitals by the pseudopotential what made the respective mathematical calculations much simpler.

For the actual purpose of atomic and molecular calculations Hellmann suggested a simple analytic formula. Let φ be the sum of electrostatic, exchange, and polarization potentials, representing the interaction between a valence electron and the core of an atom. Let φ_p be the *Abstossungspotential*. The potential $\varphi_H = \varphi + \varphi_p$ may be expressed:

$$\varphi_{ei}^H(r) = -\frac{ze^2}{4\pi\epsilon_0 r} + \frac{e^2}{4\pi\epsilon_0 r} A \exp(-\alpha r), \quad (1)$$

Here z is the ionic charge of the core; that is, if the nucleus contains Z positive charges and the core contains N electrons then $z = Z - N$. The constants A and α are determined from the requirement that the potential φ_H should reproduce the energy spectrum of the valence electron as accurately as possible. Later on several modifications were introduced by Schwarz, Bardsley etc. into the determination of the Hellmann potential parameters without changing the basic analytic form of the potential [42]. For instance, Schwarz improved the determination of the potential parameters of the second Be⁺, Mg⁺, Ca⁺, Sr⁺, Zn⁺ and first Li, Na, K, Rb, Cu periodic families considerably obtaining the better fit to the empirical energy levels [43].

However, all the mentioned above pseudopotentials have one drawback. They are usually described in \mathbf{r} space by a discontinuous function or have a relatively hard core as in a case of Hellmann potential. As a result, their Fourier transforms (formfactors) at $q \rightarrow \infty$ do not provide the sufficient convergence of series and integrals of the perturbation theory. Alternatively, Gurskii and Krasko constructed a pseudopotential model excluding the mentioned

shortcoming by introducing a continuous in \mathbf{r} space pseudopotential. On a base of smoothness of the obtained electron density distribution in an atom, Gurskii and Krasko proposed the following electron-ion model pseudopotential [31], [44]:

$$\varphi^{HGK}_{ei}(r) = -\frac{ze^2}{4\pi\epsilon_0 r} \left[1 - \exp\left(-\frac{r}{R_{Cei}}\right) \right] + \frac{ze^2}{4\pi\epsilon_0} \frac{a}{R_{Cei}} \exp\left(-\frac{r}{R_{Cei}}\right), \quad (2)$$

where $z-$ valency, $R_{Cei} = r_{Cei}r_B$ and a are determined experimentally using the ionization potential and the form-factor of the screened pseudopotential at the first sites of the reciprocal lattice. r_{Cei} is defined as a certain radius characterizing the size of the region of internal electron shells. If such measurements are not available, the second condition is replaced by the constraint that $P = 0$ at $T = 0$ in the equilibrium lattice. The magnitudes are given in SI system of units. In this work values of a , r_{Cei} are taken from [32]. One needs to make a remark that the first two terms are identical with the potential of Hellmann [27]. Due to this fact we call this pseudopotential as Hellmann-Gurskii-Krasko potential. The results of calculation of bound energy and phonon spectra with the help of Hellmann-Gurskii-Krasko (HGK) potential were found in a good agreement with the experimental data and can be used in a wide range of investigation of thermodynamic properties of Alkali plasmas. Unfortunately there are no available HGK parameters for Be^{2+} element. That is why we have found the parameters but for an alternative pseudopotential namely Fiolhais et al. [57]. The

Fiolhais potential has the following view:

$$\varphi^F_{ei}(r) = -\frac{ze^2}{4\pi\epsilon_0 r_c} \frac{1}{R} \{1 - (1 + \beta R) \exp(-\alpha R)\}, \quad (3)$$

with $R = r/r_c$, r_c being a core decay length, $\alpha > 0$, $\beta = (\alpha^3 - 2\alpha)/4(\alpha^2 - 1)$ and $A = \alpha^2/2 - \alpha\beta$. In [57] there are two possible choices of parameters - ‘‘universal’’ and ‘‘individual’’. We made a fit for the ‘‘universal’’ parameters of HGK to the Fiolhais et al., which are $a = 3.72$, $r = 0.22$. In [57] the universal parameters were chosen to obtain the best agreement between calculated and measured structure factors of Alkali metals. In the Fig. 1 the comparison between the electron-ion Fiolhais et al., HGK and Coulomb potentials for Be^{2+} plasma are shown. One can easily see that HGK almost coincided with the Fiolhais et al. potential. In the Fig. 2a one can see the comparison between the different pseudopotential of different Alkali plasmas, where by electron-ion Hellmann-Gurskii-Krasko potential the minimum appears. The Hellmann type pseudopotentials were proposed in works [33]- [35] to use for Alkali plasma.

The Hellmann-Gurskii-Krasko model for an ion-ion interaction shown in Fig. 2b for Alkali plasmas is the following:

$$\varphi^{HGK}_{ii}(r) = \frac{z^2e^2}{4\pi\epsilon_0 r} \left[1 - \exp\left(-\frac{r}{R_{Cii}}\right) \right] + \frac{z^2e^2}{4\pi\epsilon_0} \frac{a}{R_{Cii}} \exp\left(-\frac{r}{R_{Cii}}\right), \quad (4)$$

Here values of r_{Cii} , a are not given in literature. r_{Cii} is taken hypothetically as the doubled value of that taken for $e - i$ interaction $r_{Cii} = 2r_{Cei}$ taking in this way both ions cores (closed shells) into account. We will study this in more detail and compare with the hard-core potential

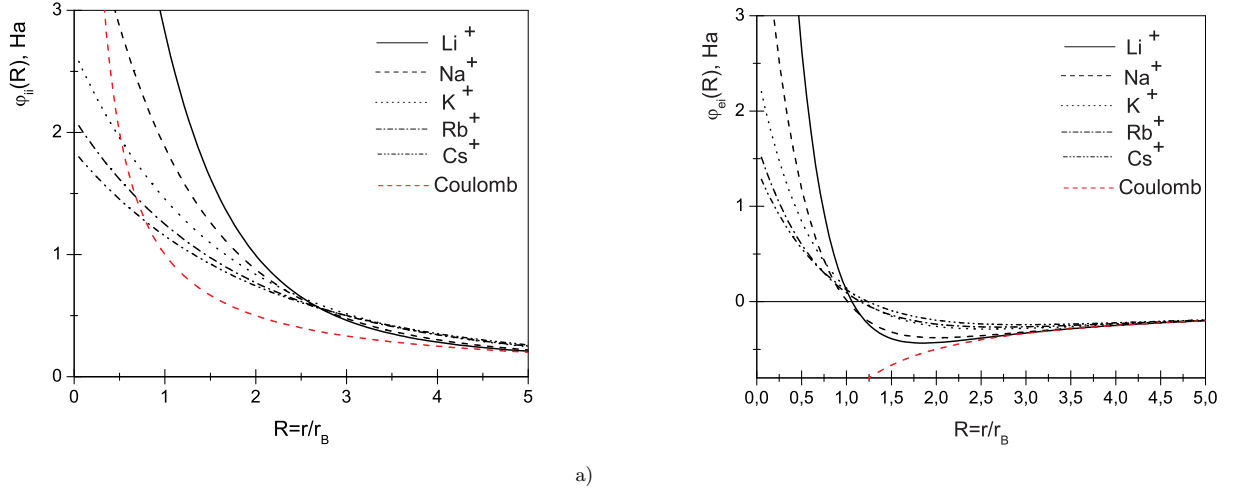


Fig. 2. Comparisons among the different HGK potentials of different Alkali plasmas. As the length scale we use the atomic system of units.

Table 2. The parameters of the Hellmann-Gurskii-Krasko potential given in a.u. Here, in the case $z = 2$ the given parameters correspond to the interaction of the double charged ion with the electron.

	Li	Na	K	Rb	Cs	Be	Mg	Ca	Sr	Br
z	1	1	1	1	1	2	2	2	2	2
a	5.954	3.362	2.671	2.293	2.214	3.72	2.588	2.745	2.575	2.870
rc_{ei}	0.365	0.487	0.689	0.779	0.871	0.22	0.427	0.571	0.644	0.698
rc_{ii}	0.73	0.974	1.948	1.558	1.742	0.44	0.854	1.142	1.288	1.396

described in [34]. In the table 2 the parameters of the Hellmann-Gurskii-Krasko potential for Alkali elements and elements of the second periodic family are presented. Here, we note that $\varphi^{HGK}_{ei}(r)$ potential describes the interaction of a valence electron with the corresponding ion core of a charge z and radius R_{Cei} , while $\varphi^{HGK}_{ii}(r)$ describes the interaction between the two ion cores of a charge z

with the common radius R_{Cii} .

In [34] it was proposed to describe the ion-ion interaction by the model of charged hard spheres with the crystallographic radii R_i . The electrical part of the ion-ion interaction is to be described by a pseudopotential:

$$\varphi^{HC}_{ii}(r) = \begin{cases} \frac{ze^2}{4\pi\epsilon_0 r}, & r > 2R_i \\ \infty, & r < 2R_i \end{cases} \quad (5)$$

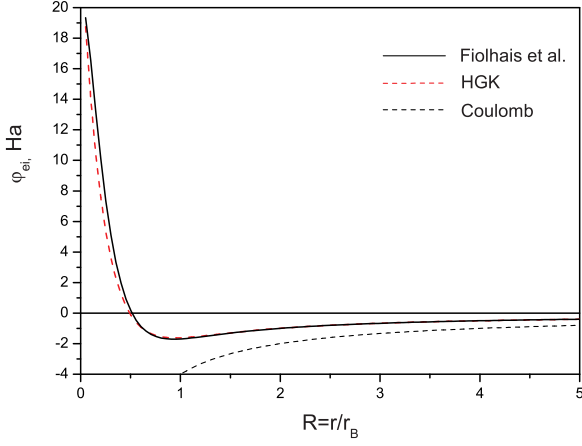


Fig. 1. Comparisons among the $e-i$ HGK, Fiolhais et al. and Coulomb potentials for (a) Be^{2+} . As the length scale we use the atomic system of units.

In principle the choice of the parameters for the ion-ion interaction should be based on methods similar to those in [32]. As a simple approximation we propose to use the crystallographic ion radii R_i [45] in the first constituent of the potential:

$$\varphi^{SC}_{ii}(r) = \frac{z^2 e^2}{4\pi\epsilon_0 r} \left[1 - \exp\left(-\frac{r}{R_i}\right) \right] + \frac{z^2 e^2}{4\pi\epsilon_0} \frac{a}{R_{Cii}} \exp\left(-\frac{r}{R_{Cii}}\right), \quad (6)$$

Furthermore, on a base of our calculations we came to the conclusion that the potential is not sensitive with respect to the a parameter of the ion-ion interaction. That is why a is taken the same as for electron-ion interaction. In the Figure 3a, b the comparison between the HGK model and Hard Core (HC) model is shown.

The pseudopotentials which are used in our calculations were originally developed for applications in the electronic band structure and binding energies in Alkali metals. However the derivation used by Hellmann and his fol-

lowers is basically working with wave functions of a few particles and not N -particle wave functions of the solid state. For this reason we can not see strong arguments against applications to the two-particle interactions in the plasma state. Of course this is a working assumption which needs further justification. Anyhow we are convinced that application of pseudopotentials of Hellmann-type is much nearer to reality than the use of pure Coulomb potentials or hard-core potentials. Further we would like to argue that the experimental investigations of Alkali metals near to the critical point did not show the existence of deep differences between the two particle interactions in the liquid and the gaseous state [1], [2]. What is clearly different are the multi-particle interactions, however multi-particle effects are less relevant at the densities we consider here.

2.1 Screening of the Hellmann-Gurskii-Krasko potential

To determine the thermodynamic and transport properties of semiclassical fully ionized plasma effective potentials simulating quantum effects of diffraction and symmetry [20] - [24] and later significantly improved potentials [25,26] are widely used. In particular, Deutsch and co-workers [46], [47] have obtained the following form of effective interaction potential of charged particles in plasma medium:

$$\varphi_{ee} = \frac{e^2}{4\pi\epsilon_0 r} \left[1 - \exp\left(-\frac{r}{\lambda_{ee}}\right) \right] + k_B T \ln 2 \exp\left(-\frac{r^2}{\lambda_{ee}^2 \ln 2}\right), \quad (7)$$

where e is the electric elementary charge, $\lambda_{ee} = \hbar/\sqrt{m_e k_B T}$ is the electron thermal de-Broglie wavelength. The pseu-

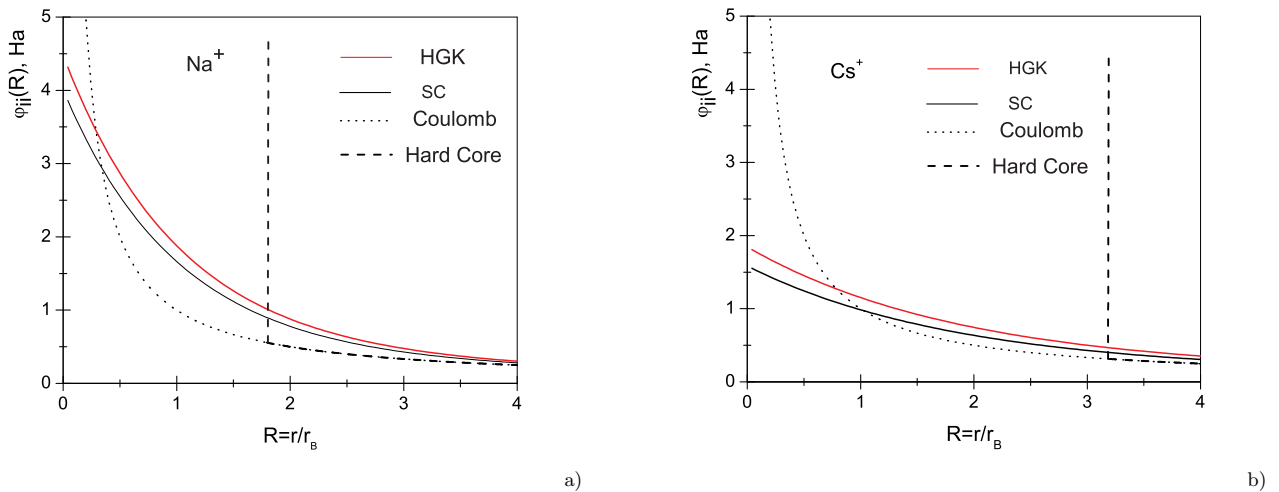


Fig. 3. Comparisons among the $i - i$ HGK, Hard Core, Soft Core and Coulomb potentials for (a) Na^+ and (b) Cs^+ plasmas. As the length scale we use the atomic system of units.

dopotential (7) does not take into account collective events in plasmas. In the works [38], [39] it was proposed to use the $e - e$ effective potential (7), corresponding $e - i$ and $i - i$ potentials at short distances and the screened potential, treating three particle correlations at large ones. The transition from one potential curve to another was realized at the intersection point by the spline-approximation method.

The pseudopotential model (7) was developed only for highly ionized plasmas. Since most experimental data available refer to partially ionized plasmas at moderate temperatures when the ions partially retain their inner shell, it is of a high interest to construct the pseudopotential model which takes into account not only the quantum-mechanical and screening field effects but also the ion shell structure. In order to include the screening effects, in previous work [13], we applied the method developed in [37]

and [39]. In [39] the authors developed the classical approach based on the chain of Bogoljubow equations [36] for the equilibrium distribution functions where the potential (7) was taken as a micropotential. In our paper [13] we derived the Fourier transforms of the screened HGK eq. (11)-(14) therein using the $e - i$, $i - i$ Hellmann-Gurskii-Krasko pseudopotentials (2), (4) and $e - e$ Deutsch potential (7) as micropotentials.

In the work [13] there was obtained the following screened HGK : In Fourier space this system of integral-differential equations turns into a system of linear algebraic equations:

$$\Phi_{ab}(k) = \varphi_{ab}(k) - \frac{1}{k_B T} [n_e \varphi_{ae}(k) \Phi_{eb}(k) + n_i \varphi_{ai}(k) \Phi_{ib}(k)] \quad (8)$$

where $a, b = i, e$. Solving the system (8) for two-component plasma one can derive the following expressions for the Fourier transform $\Phi_{ab}(k)$ of the pseudopotential $\Phi_{ab}(r)$:

$$\Phi_{ei}(k) = \frac{Ze^2}{\varepsilon_0 \Delta} \frac{(2a - 1) R_{cei}^2 k^2 - 1}{k^2 (1 + k^2 R_{cei}^2)^2}, \quad (9)$$

$$\begin{aligned} \Phi_{ee}(k) &= \frac{e^2}{\varepsilon_0 \Delta} \left\{ \frac{1}{k^2(1+k^2\lambda_{ee}^2)} \right. \\ &+ \frac{1}{k^4 r_{De}^2} \left[\frac{(2a+1)R_{c_{ii}}^2 k^2 + 1}{(1+k^2\lambda_{ee}^2)(1+k^2 R_{c_{ii}}^2)^2} - \left(\frac{(2a-1)R_{c_{ei}}^2 k^2 - 1}{(1+k^2 R_{c_{ei}}^2)^2} \right)^2 \right] \\ &\left. + A \left(1 + \frac{(2a+1)R_{c_{ii}}^2 k^2 + 1}{k^2 r_{Di}^2 (1+k^2 R_{c_{ii}}^2)^2} \right) \exp\left(-\frac{k^2}{4b}\right) \right\}, \quad (10) \end{aligned}$$

$$\begin{aligned} \Phi_{ii}(k) &= \frac{Z^2 e^2}{\varepsilon_0 \Delta} \left\{ \frac{(2a+1)R_{c_{ii}}^2 k^2 + 1}{k^2(1+k^2 R_{c_{ii}}^2)^2} \right. \\ &+ \frac{1}{k^4 r_{De}^2} \left[\frac{(2a+1)R_{c_{ii}}^2 k^2 + 1}{(1+k^2\lambda_{ee}^2)(1+k^2 R_{c_{ii}}^2)^2} - \left(\frac{(2a-1)R_{c_{ei}}^2 k^2 - 1}{(1+k^2 R_{c_{ei}}^2)^2} \right)^2 \right] \\ &\left. + A \frac{(2a+1)R_{c_{ii}}^2 k^2 + 1}{k^2 r_{De}^2 (1+k^2 R_{c_{ii}}^2)^2} \exp\left(-\frac{k^2}{4b}\right) \right\}, \quad (11) \end{aligned}$$

here r_{De} , r_{Di} are the Debye radius of electrons and ions respectively, where $1/r_{Di}^2 = Z^2 e^2 n_i / (\varepsilon_0 k_B T)$,

$$1/r_{De}^2 = e^2 n_e / (\varepsilon_0 k_B T), \quad b = (\lambda_{ee}^2 \ln 2)^{-1},$$

$A = k_B T \ln 2 \pi^{3/2} b^{-3/2} \varepsilon_0 / e^2$ and Δ is:

$$\begin{aligned} \Delta &= 1 + \frac{1}{k^2 r_{De}^2 (1+k^2\lambda_{ee}^2)} + \frac{(2a+1)R_{c_{ii}}^2 k^2 + 1}{k^2 r_{Di}^2 (1+k^2 R_{c_{ii}}^2)^2} \\ &+ \frac{1}{k^4 r_{De}^2 r_{Di}^2} \left[\frac{(2a+1)R_{c_{ii}}^2 k^2 + 1}{(1+k^2\lambda_{ee}^2)(1+k^2 R_{c_{ii}}^2)^2} - \left(\frac{(2a-1)R_{c_{ei}}^2 k^2 - 1}{(1+k^2 R_{c_{ei}}^2)^2} \right)^2 \right] \\ &+ \frac{A}{r_{De}^2} \left(1 + \frac{(2a+1)R_{c_{ii}}^2 k^2 + 1}{k^2 r_{Di}^2 (1+k^2 R_{c_{ii}}^2)^2} \right) \exp\left(-\frac{k^2}{4b}\right) \quad (12) \end{aligned}$$

The pseudopotential $\Phi_{ab}(r)$ can be restored from (9-12) by Fourier transformation

$$\Phi_{ab}(r) = \frac{1}{2\pi^2 r} \int \Phi_{ab}(k) k \sin(kr) dk \quad (13)$$

The present approximation is restricted to the constraint $\Gamma \lesssim 1$ due to the use of linearisation process at the derivation of the solved integral-differential equation .

In the Figure 4 the $e-i$ and $i-i$ HGK and screened HGK and $i-i$ S.S. Dalgic et al. potentials are presented for comparison. One can easily see that with increasing of Γ the curves shift in the direction of its low absolute values due to the increasing role of the screening effects.

As we have stressed above there is no available parameter for the ion-ion interaction potential 4. That is why we have looked for alternative pseudopotentials. One of

them is the screened ion-ion potential determined by S. S. Dalgic et al. [58] on a base of the second order pseudopotential perturbation theory using the Fiolhais et al. potential $\varphi_{ei}^F(r)$:

$$\Phi_{ii}^D(k) = \frac{4\pi Z^2 e^2}{4\pi \varepsilon_0 k^2} + \chi(k) |\varphi_{ei}^F(k)|^2, \quad (14)$$

where $\varphi_{ei}^F(k)$ is the pseudopotential local form factor. In the present work we use instead the HGK $\Phi_{ii}^{HGK}(k)$ potential with the fitted to Fiolhais et al. potential parameters. $\chi(k)$ is the response of the electron gas:

$$\chi(k) = \frac{\chi^0(k)}{1 - \left(\frac{4\pi e^2}{4\pi \varepsilon_0 k^2}\right) [1 - G(k)] \chi^0(k)}, \quad (15)$$

where $\chi^0(k)$ is the Lindhard response of a non-interacting degenerated electron gas.

$$\chi^0(k) = -\frac{k_F m_e}{2\pi^2 \hbar^2} \left[1 + \frac{1-x^2}{2x} \ln \left| \frac{1+x}{1-x} \right| \right], \quad (16)$$

and $G(k)$ is the local field correction (LFC), which accounts for the interactions between the electrons. For its determination we used a LFC which satisfies the compressibility sum rule at finite temperatures obtained by Gregori et al. for strong coupling regimes [15].

2.2 Static Structure Factor

Within the framework of the density response formalism for a two component plasma, we can calculate the screened HGK interaction potentials using the semiclassical approach suggested by Arkhipov and Davletov [39], which is based on a HGK pseudopotential model for the interaction between charged spheres-particles to account for ion structure, quantum diffraction effects i.e., the Pauli

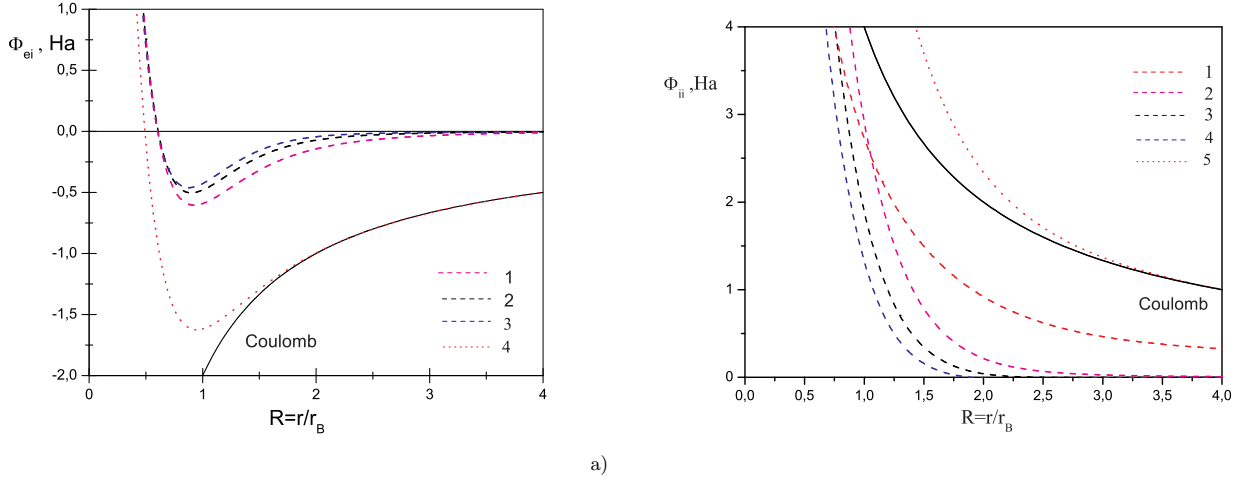


Fig. 4. The screened e-i HGK Φ_{ei} and i-i HGK Φ_{ii} for Beryllium plasma (Be^{2+}). a) 1: Screened HGK at $T_e = T_i = 40eV, T'_e = 42.17eV, \Gamma_{ee} = 0.346$; 2: Screened HGK at $T_e = T_i = 20eV, T'_e = 24.06eV, \Gamma_{ee} = 0.606$, 3: Screened HGK at $T_e = T_i = 13eV, T'_e = 18.65, \Gamma_{ee} = 0.782$, 4: HGK; b) 1: S.S. Dalgic et al. at $T_e = T_i = 13eV, T'_e = 18.65, \Gamma_{ee} = 0.782$; 2: Screened HGK at $T_e = T_i = 40eV, T'_e = 42.17eV, \Gamma_{ee} = 0.346$; 3: Screened HGK at $T_e = T_i = 20eV, T'_e = 24.06eV, \Gamma_{ee} = 0.606$; 4: Screened HGK at $T_e = T_i = 13eV, T'_e = 18.65, \Gamma_{ee} = 0.782$, 5: HGK. As the length scale we use the atomic system of units.

exclusion principle and symmetry. Quantum diffraction is represented by the thermal de Broglie wavelength $\lambda_{rs} = \hbar/\sqrt{2m_{rs}k_B T'_{rs}}$ with $\mu'_{rs} = \frac{m_r m_s}{m_r + m_s}$ the reduced mass of the interacting pair $r - s$, and $r, s = e$ (electrons) or i (ions). The effective temperature T'_{rs} is given by ,

$$T'_{rs} = \frac{m_r T'_s + m_s T'_r}{m_r + m_s},$$

where $T'_e = (T_e^2 + T_q^2)^{1/2}$ with $T_q = T_F/(1.3251 - 0.1779\sqrt{r_s})$, $r_s = r_a/r_B$ and $T'_i = (T_i^2 + \gamma_0 T_D^2)^{1/2}$, $T_D = \Omega_{pi}\hbar/k_B$ is the Bohm-Staver relation for Debye temperature with $\Omega_{pi}^2 = \omega_{pi}^2/(1 + k_{De}/k^2)$, $\omega_{pi} = \sqrt{ze^2 n_e/(\epsilon_0 m_i)}$ with m_i ion mass, $k_{De} = \sqrt{e^2 n_e/(\epsilon_0 k_B T'_e)}$ is the Debye wave number for the electron fluid ($T_D \approx 0.16eV, T_F \approx 14.5eV$ for Be^{2+}). Since, in the Debye model, phonon modes with

wavelength up to a fraction of the lattice spacing are considered, in [14] it is set $k \equiv k_{max} = (2/z)^{1/3} k_F$ with $k_F = (3\pi^2 n_e)^{1/3}$ Fermi wave number. Due to the large mass difference between ions and electrons, $T'_{ei} = T'_{ee}$. All the parameters considered here are beyond the degeneration border ($n_e \lambda_{ee}^3 < 1$).

As described in [14] by Gregori et al. the fluctuation-dissipation theorem may be still a valid approximation even under nonequilibrium conditions if the temperature relaxation is slow compared to the electron density fluctuation time scale. A common condition in experimental plasmas for this to occur is when $m_i \gg m_e$ so that the coupling between the two components takes place at sufficiently low frequency. Using a two-component hypernetted chain (HNC) approximation scheme, Seuferling et al.

[16] have shown that the static response under non-Local Thermodynamic Equilibrium (LTE) takes the form:

$$S_{rs}(k) = \delta_{rs} - \frac{\sqrt{n_r n_s}}{k_B T'_{rs}} \Phi_{rs} - \delta_{er} \delta_{es} \left(\frac{T'_e}{T'_i} - 1 \right) \frac{|q(k)|^2}{z} S_{ii}(k) \quad (17)$$

where $q(k) = \sqrt{z} S_{ei}(k) / S_{ii}(k)$ and for Φ_{rs} the expression (9-12) have been used.

In the Figures 5 (a), (b), (c), (d) the static structure factors S_{rs} (SSF) in dependence on k_{De} for a Beryllium plasma with the introduced above different temperatures $T_i = T_e$, $T_i = 0.5 \cdot T_e$, $T_i = 0.2 \cdot T_e$ and coupling parameter $\Gamma_{ee} = e^2 / (4\epsilon_0 k_B T'_e r_{ee})$, $\Gamma_{ii} = z^2 e^2 / (4\epsilon_0 k_B T'_i r_{ii})$ with $r_{ii} = (3/4\pi n_i)^{1/3}$, $r_{ee} = (3/4\pi n_e)^{1/3}$ are shown. For typical conditions found in laser plasma experiments with solid density beryllium, we have $n_e \approx 2.5 \cdot 10^{23} \text{cm}^{-3}$ and $z \approx 2$. This gives $T_F \approx 14.5 \text{eV}$ and $T_D \approx 0.17 \text{eV}$. In the Figure 5 (c) a minimum arises which defines the size of an ion core. One can see that in the Figure with increasing of Γ one can notice that a minimum becomes less pronounced.

In the Figure 5 (a) S_{ii} , shown as the blue line, was determined with the help of potential (14) described above. On a base of this potential described by Dalgic et al. E. Apfelbaum calculated SSF of Cs and Rb in the region of liquid-plasma transition [59]. The author showed that calculated data were in agreement with the measured SSF. In a screened OCP the effective response of the medium is described by the charge-charge correlation function [51]:

$$S_{zz}(k) = \frac{(S_{ee} + Z S_{ii} - 2\sqrt{Z} S_{ei})}{1 + Z} \quad (18)$$

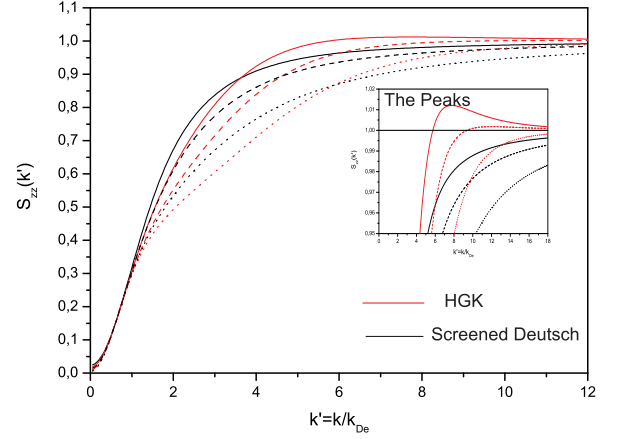


Fig. 6. The charge-charge static structure factors S_{zz} for a beryllium plasma with $n_e \approx 2.5 \cdot 10^{23} \text{cm}^{-3}$, $z \approx 2$, and $T_e = 20 \text{eV}$, $T'_e = 24.06 \text{eV}$. Black set of lines represents the screened Deutsch model obtained here on a base of Gregori et al. [14], while the red one - the screened HGK model. Solid line: $T_i/T_e = 1$ ($\Gamma_{ii} = 2.31$, $\Gamma_{ee} = 0.61$). Dashed line: $T_i/T_e = 0.5$ ($\Gamma_{ii} = 4.63$, $\Gamma_{ee} = 0.61$). Dotted line: $T_i/T_e = 0.2$ ($\Gamma_{ii} = 11.57$, $\Gamma_{ee} = 0.61$).

It is of high interest to study the influence of the ion structure on the static structure factors. For this reason in the Figures 5 (a)-(d) and further on we compare the SSF, obtained from equations (17) and (18) with the help of the screened HGK potentials (9-12), with the corresponding SSF obtained with the help of the screened Deutsch potential [39], on a base of the modified RPA developed by Gregori et al. [14] where no ion structure is taken into account.

In the Figure 6 the static charge-charge structure factor for a beryllium plasma with $n_e \approx 2.5 \cdot 10^{23} \text{cm}^{-3}$, $z \approx 2$, $T_e = 20 \text{eV}$ and $T_i = T_e$, $T_i = 0.5 \cdot T_e$, $T_i = 0.2 \cdot T_e$ is shown. In the Figure 7 (a) - (d) we compare our results

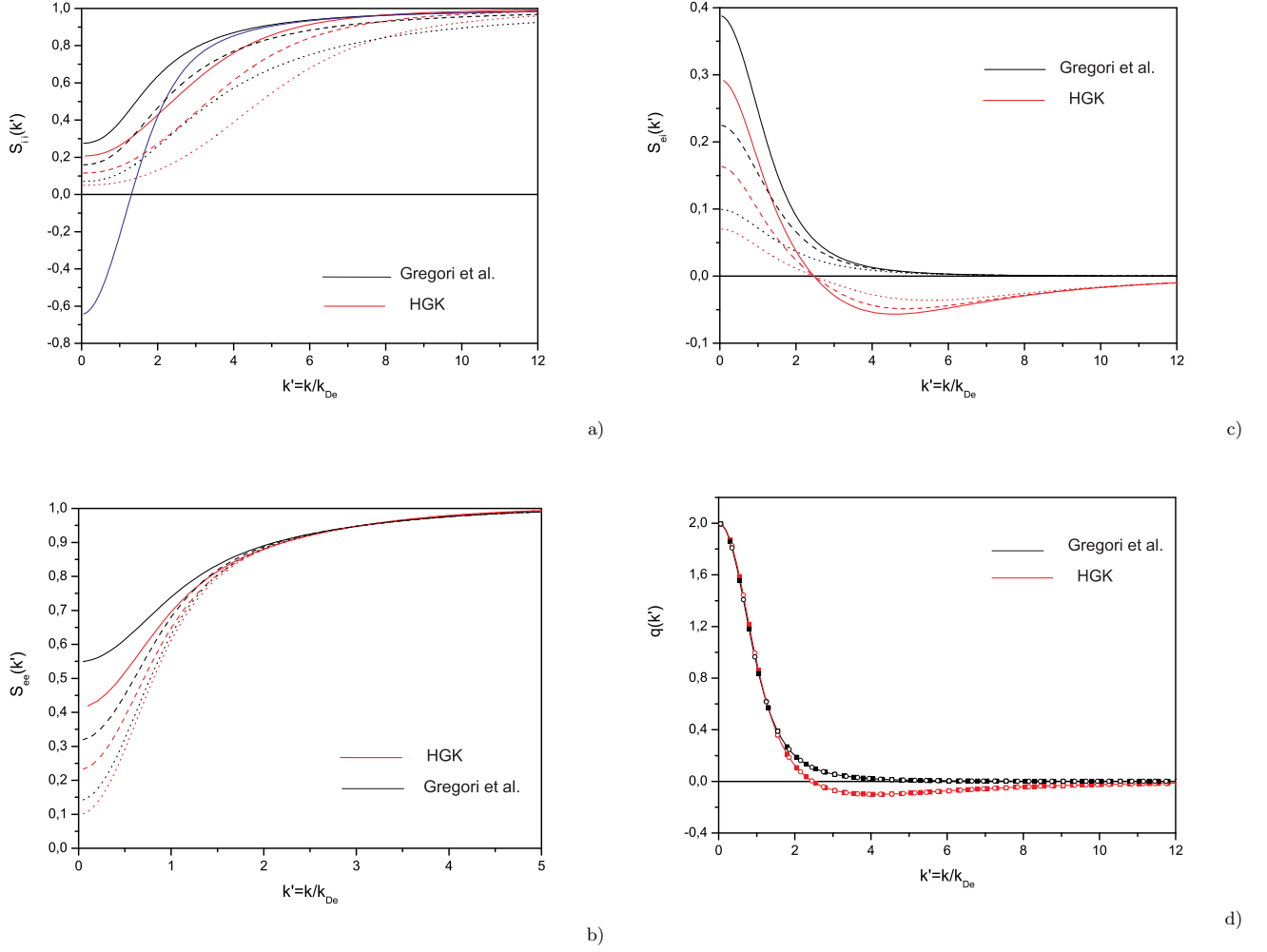


Fig. 5. Static structure factors and screening charge $q(k')$ for Be^{2+} plasma at $T_e = 20eV$, $T_e' = 24.06eV$, $Z = 2$ and $n_e = 2.5 \times 10^{23} cm^{-3}$. Black set of lines represents the screened Deutsch model obtained by Gregori et al.[14], while the red one - the screened HGK model. Solid line: $T_i/T_e = 1$ ($\Gamma_{ii} = 2.31$, $\Gamma_{ee} = 0.61$). Dashed line: $T_i/T_e = 0.5$ ($\Gamma_{ii} = 4.63$, $\Gamma_{ee} = 0.61$). Dotted line: $T_i/T_e = 0.2$ ($\Gamma_{ii} = 11.57$, $\Gamma_{ee} = 0.61$). (a) The blue solid line: SSF calculated according to the eq.(17) with (14). (d) The solid line: $T_i/T_e = 1$. The filled squares: $T_i/T_e = 0.5$. The hollow circles: $T_i/T_e = 0.2$.

of charge-charge SSF for Alkali plasmas with the results obtained in the present work for Alkali (Hydrogen-like) plasmas considered in a frame of the screened Deutsch model at the various densities and temperatures. All the curves obtained in a frame of the screened Deutsch model converge due to the negligible influence of an ion mass on λ_{ab} entering the equations. As one can easily see with an

increase of Γ the peaks become more pronounced and the difference among curves becomes significant. We see that strong coupling and the onset of short-range order appear in S_{zz} as a first localized peak, shown in a amplified scale, at the different k' for every Alkali species and the position of the peaks shifts in a direction of the small k' value. This

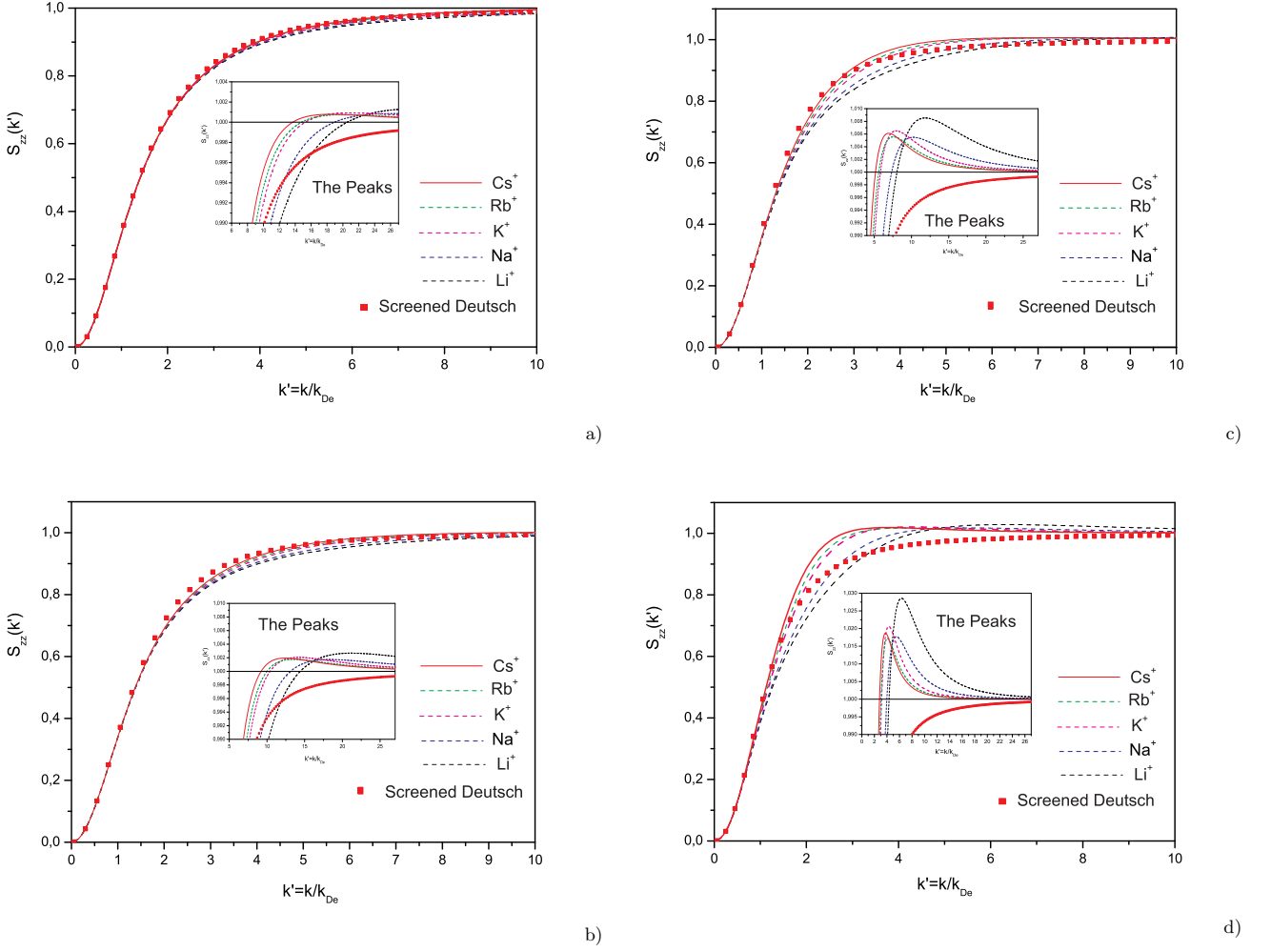


Fig. 7. The charge-charge static structure factors S_{zz} for Alkali plasmas (Li^+ , Na^+ , K^+ , Rb^+ , Cs^+) in a frame of the screened HGK model and results obtained in the present work for Hydrogen-like plasmas in a frame of the screened Deutsch model on a base of Gregori et al.[14]. (a) $T_e = T_i = 60000\text{K}$, $T'_e = 60204\text{K}$, $\Gamma_{ee} = 0.398$, $\Gamma_{ii} = 0.399$; (b) $T_e = T_i = 30000\text{K}$, $T'_e = 30407\text{K}$, $\Gamma_{ee} = 0.789$, $\Gamma_{ii} = 0.8$; (c) $T_e = T_i = 30000\text{K}$, $T'_e = 31471\text{K}$, $\Gamma_{ee} = 1.14$, $\Gamma_{ii} = 1.2$; (d) $T_e = T_i = 30000\text{K}$, $T'_e = 37806\text{K}$, $\Gamma_{ee} = 1.58$, $\Gamma_{ii} = 2$. As the length scale we use the inverse electron Debye radius.

phenomenon was also reported in [15].

3 Dynamic Structure Factor. Method of Moments

Extensive molecular-dynamic simulations of a Coulomb system over a wide range of plasma parameters Γ and

$\Theta = E_F/k_B T$ (E_F is the Fermi energy) have been carried out by Hansen et al [51]. Hansen et al. studied dynamic and static properties of OCP and TCP plasmas and binary ionic systems. In the work of V. M. Adamjan, et al. [52], [53] a new “method of moments” based on exact relations and sum rules for calculating of dynamical characteristics of OCP and of the charge-charge dynamic structure factor

for the model semiquantal two-component plasma (TCP) was proposed. The “method of moments” proved to produce the best agreement with the MD data of Hansen et al. The dynamic structure factor $S_{zz}(k, \omega)$ is defined via the fluctuation-dissipation theorem (FDT) as

$$S_{zz}(k, \omega) = -\frac{\hbar \Im \varepsilon^{-1}(k, \omega)}{\pi \Phi(k) [1 - \exp(-\beta \hbar \omega)]}, \quad (19)$$

where $\Phi(k) = e^2/\varepsilon_0 k^2$, \hbar is the reduced Planck constant and $\varepsilon^{-1}(k, \omega)$ is the inverse longitudinal dielectric function of the plasma. In order to construct the inverse longitudinal dielectric function one needs to consider the frequency moments of the loss function $-\Im \varepsilon^{-1}(k, \omega)/\omega$:

$$C_\nu(k) = -\pi^{-1} \int_{-\infty}^{\infty} \omega^{\nu-1} \Im \varepsilon^{-1}(k, \omega) d\omega, \quad (20)$$

The Nevanlinna formula of the classical theory of moments [54] expresses the response function

$$\varepsilon^{-1}(k, \omega) = 1 + \frac{\omega_p^2(\omega + q)}{\omega(\omega^2 - \omega_2^2) + q(\omega^2 - \omega_1^2)}, \quad (21)$$

in terms of an R-function $q = q(k, \omega)$. The frequencies ω_1 and ω_2 are defined as respective ratios of the moments C_ν ,

$$\begin{aligned} \omega_1^2 &= C_2/C_0 = \omega_p^2 [1 - \varepsilon^{-1}(k, 0)]^{-1}, \\ \omega_2^2 &= C_4/C_2 = \omega_p^2 [1 + Q(k)], \end{aligned} \quad (22)$$

where $\varepsilon^{-1}(k, 0)$ can be determined from the classical form ($\hbar \rightarrow 0$) of the FDT (thermal equilibrium) eq. (19) and the Kramers-Kronig relation [55]:

$$\Re \varepsilon^{-1}(k, \omega) = 1 + \frac{1}{\pi} P.V. \int_{-\infty}^{\infty} \frac{\Im \varepsilon^{-1}(k, \omega')}{\omega' - \omega} d\omega' \quad (23)$$

In this way, we get the following expression :

$$\Re \varepsilon^{-1}(k, 0) = 1 - 2S_{zz} \frac{k_{De}^2}{k^2}, \quad (24)$$

where $\Re \varepsilon^{-1}(k, 0) = \varepsilon^{-1}(k, 0) = \varepsilon^{-1}(k)$, and

$$\begin{aligned} S_{zz}(k) &= \frac{1}{n_e + Zn_i} \int_{-\infty}^{\infty} S_{zz}(k, \omega) d\omega \\ &= \frac{S_{ee} - 2\sqrt{Z} S_{ei} + Z S_{ii}}{2}, \end{aligned} \quad (25)$$

where $T'_e = T'_i = T_e = T$, $T'_{ei} = T'_{ee} = T'_e$, $n_e = Zn_i$.

$$Q(k) = K(k) + L(k) + H \quad (26)$$

represents the TCP correction with the kinetic contribution for a classical system

$$K(k) = 3\left(\frac{k}{k_D}\right)^2, \quad (27)$$

where $k_D^2 = k_{De}^2 = k_{Di}^2 = 4\pi n_e e^2/k_B T$ ($n_e = n_i$) the contribution due to electron-ion HGK correlations,

$$H = \frac{1}{6\pi^2 \sqrt{n_e n_i}} \int_0^\infty p^2 S_{ei}(p) \zeta_{ei} dp, \quad (28)$$

with $\Phi_{ab}(k) = \Phi(k) \zeta_{ab}(k)$, $\alpha, \beta = e, i$ given in (9-12) and

$$L(k) = \frac{1}{2\pi^2 n_e} \int_0^\infty p^2 [S_{ee}(p) - 1] f(p, k) dp, \quad (29)$$

which takes into account the electronic correlations,

$$f(p, k) = \int_{-1}^1 \frac{(ps-k)^2}{p^2 - 2psk + k^2} \zeta_{ee}(\sqrt{p^2 - 2pks + k^2}) \frac{ds}{2} - \frac{\zeta_{ee}(p)}{3}, \quad (30)$$

In the equations (28), (29) the static structure factor is defined in (17) with the potentials given in (9-12). The authors suggested to approximate $q(k, \omega)$ by its static value $q(k, 0) = ih(k)$, connected to the static value $S_{zz}(k, 0)$ of the dynamic structure factor through eq. (19),

$$h(k) = \frac{(\omega_2^2 - \omega_1^2) \omega_p^2}{\pi \beta \phi(k) \omega_1^4 S_{zz}(k, 0)}, \quad (31)$$

with

$$S_{zz}(k, 0) = S_{zz}^0(k, 0) |\varepsilon^{-1}(k, 0)|^2, \quad (32)$$

where $S_{zz}^0(k, 0) = \frac{n_e}{k} \sqrt{\frac{m}{2\pi k_B T}}$ [56] so that the normalized dynamic factor gets the following form:

$$\frac{S_{zz}(k, \omega)}{S_{zz}(k, 0)} = \frac{\beta \hbar}{[1 - \exp(-\beta \hbar \omega)]} \times \frac{\omega h^2(k) \omega_1^4}{\omega^2(\omega^2 - \omega_2^2) + h^2(k)(\omega^2 - \omega_1^2)}, \quad (33)$$

with the more simplified expressions for $h(k)$:

$$h(k) = \frac{\varepsilon_0 k^7 \omega_p^2 (\omega_2^2 - \omega_1^2)}{\pi \beta n_e e^2 \omega_1^4 \sqrt{\frac{m}{2\pi k_B T} (k^2 - S_{zz}(k) k_{De}^2)^2}}, \quad (34)$$

$\omega_1(k)$, $\omega_2(k)$:

$$\begin{aligned} \omega_1^2 &= C_2/C_0 = \frac{\omega_p^2 k^2}{k_{De}^2 S_{zz}(k)}, \\ \omega_2^2 &= C_4/C_2 = \omega_p^2 [1 + K(k) + L(k) + H], \end{aligned} \quad (35)$$

The Figure 8 shows the behaviour of h , w_1 , w_2 given for Na^+ plasma.

As one can see in the Figures 10, 11 the curves for Alkali plasmas are different from those given for Hydrogen-like (Coulomb) model of Adamjan et al., where the ion structure is not taken into account. In a case of Alkali plasma the curves split. This can be explained by that fact that Alkali ion structure influences the dynamic structure factor. In the Figure 10 (a) the position of peaks almost coincides but the intensity in Alkali plasma is damped. We presume that the curves shift in the direction of high k compared to the Adamjan's curves. In the Figure 11 (b) the position of the second peak $\omega \approx 1.2$ is different and shifted in a low ω direction, while the intensity is shifted in a low k direction compared to the Adamjan's curves. The Na^+ curve has three peaks compared to the rest curves. At small Γ and higher k or higher Γ and lower k the difference between the present curves and the curves obtained by Adamjan et al. becomes drastic. In the Figure

10 (b) the curve for K^+ splits into two very sharp peaks, the curve for Rb^+ , Cs^+ into three while the Na^+ curve has only one wide peak. With an increase of outer electrons from K^+ the intensity decreases and the curves shift from each other. In the Figure 11 (a) the position of peaks shift in a direction of low absolute value of ω and the intensity grows with an increase of number of outer electrons. This discrepancy could be also explained by that fact that the considered parameters are extreme, i. e. either high temperature or density and for $\Gamma = 0.5$, $r_s = 0.4$ the degeneration condition is $n_e \lambda_{ee} = 0.335$, while for $\Gamma = 2$, $r_s = 1$ the degeneration condition is $n_e \lambda_{ee} = 0.678$.

In the Figures 12 and 13 the dynamic SF at the moderate temperatures $T = 30000\text{K}$ and concentrations $n_e = 1.741 \cdot 10^{20} - 10^{22} \text{cm}^{-3}$ but providing the same Γ are shown.

Now, lets us consider the different definition of the described above the H function in eq. (28):

$$H = \frac{h_{ei}(r=0)}{3} = \frac{g_{ei}(r=0) - 1}{3}, \quad (36)$$

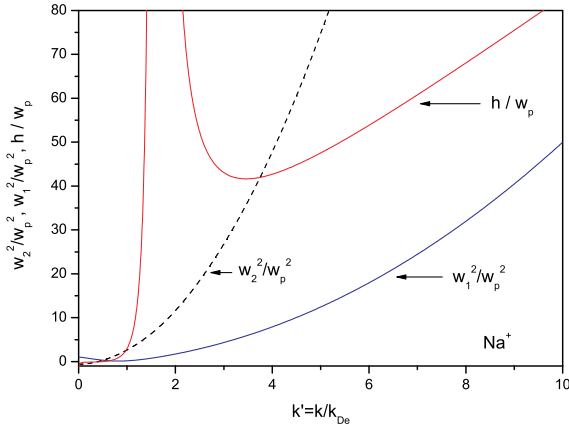
and $L(k)$, where the $f(p, k)$ function in eq. (29) will change

$$f'(p, k) = \int_{-1}^1 \frac{(ps - k)^2}{p^2 - 2psk + k^2} \zeta_{ee}(\sqrt{p^2 - 2pks + k^2}) \frac{ds}{2} - \frac{\zeta'_{ee}(p)}{3}, \quad (37)$$

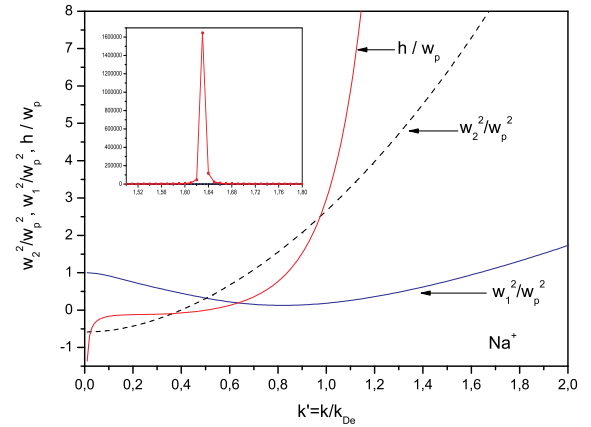
where $\zeta'_{ee}(p)$ is to be determined from eq. (7) and the following like it was made in [55]:

$$\varphi_{ee}(p) = \Phi(p) \zeta'_{ee}(p), \quad (38)$$

In a frame of the screened HGK model the H in eq. (36) will turn into $-1/3$ because we consider the ion structure, that means that the electron can not approach ion

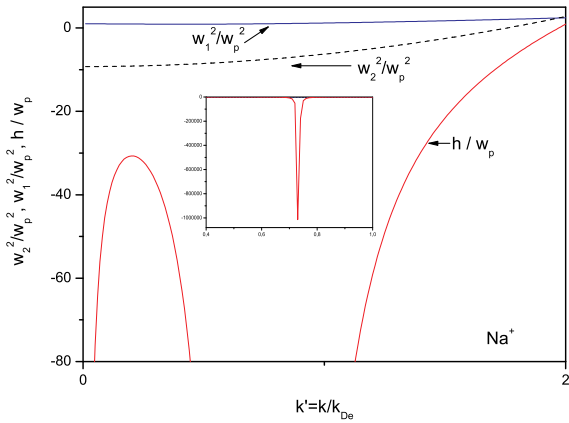


a)

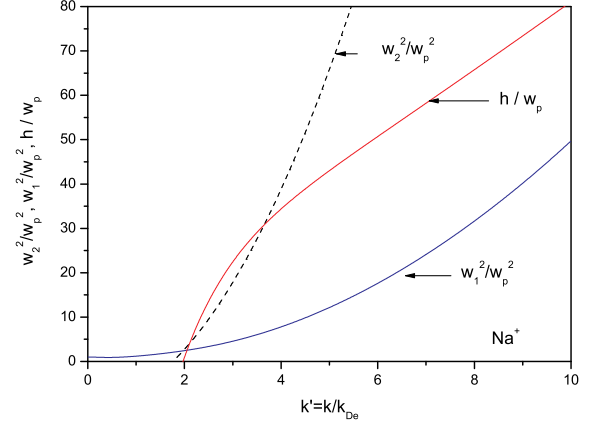


b)

Fig. 8. The h/w_p , w_1^2/w_p^2 , w_2^2/w_p^2 for Na^+ plasma at $T = 157457.3526K$, $n_e = 1.6110^{24}cm^{-3}$, $\Gamma_{ee} = 2$, $r_s = 1$, $\omega_p = n_e e^2 / \epsilon_0 m_e$.



a)



b)

Fig. 9. The h/w_p , w_1^2/w_p^2 , w_2^2/w_p^2 for Na^+ plasma at $T = 30000K$, $n_e = 1.11 \cdot 10^{22}cm^{-3}$, $\Gamma_{ee} = 2$, $r_s = 5.24$, $\omega_p = n_e e^2 / \epsilon_0 m_e$.

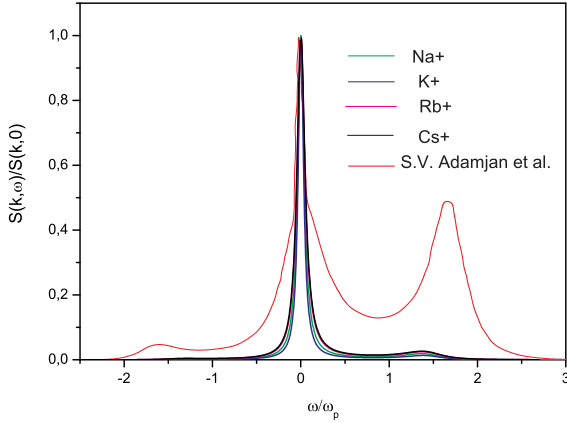
at $r = 0$ distance. If we take all this into account then we will get the plots shown in 14-15. Having compared the 12 (b) with the 14 (b) one can notice the drastic difference between the Figures and slight difference among the rest Figures, meaning that H, L definition influences the Figures.

4 Conclusions

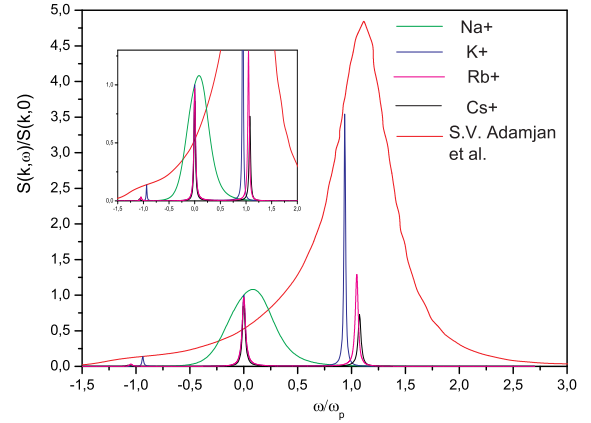
The work has been fulfilled at the Humboldt University at Berlin (Germany).

References

1. F. Hensel, *Liquid Metals*, 1976, ed. by R. Evans and D. A. Greenwood, IOP Conf. Ser. No. 30, (IPPS, London, 1977).

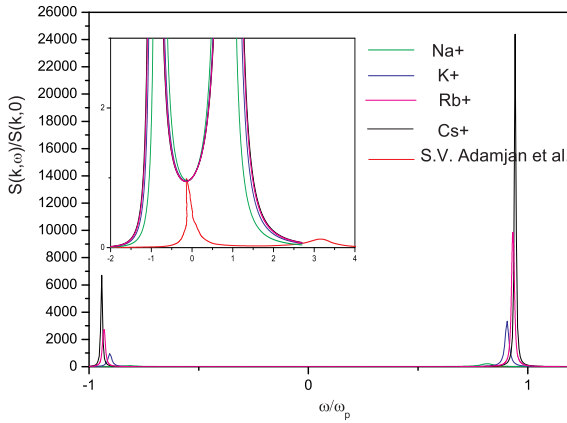


a)

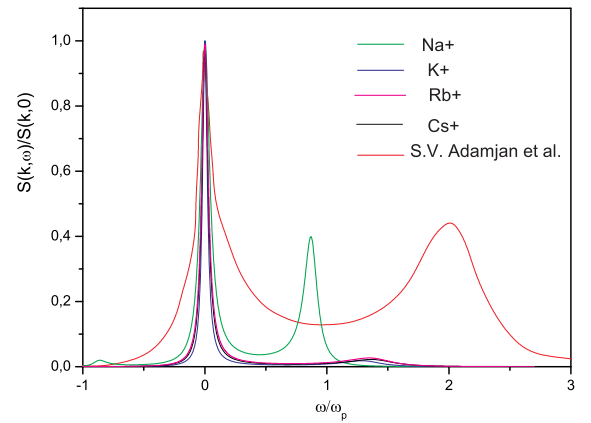


b)

Fig. 10. Comparisons among the normalised dynamic structure factor of Alkali plasmas (Na^+ , K^+ , Rb^+ , Cs^+) and results obtained by S. Adamjan et al. [53] at $k = 0.767 \cdot r_{ee}$, (a) $T = 1574573.526\text{K}$, $n_e = 2.5 \cdot 10^{25}\text{cm}^{-3}$, $\Gamma_{ee} = 0.5$ and (b) $T = 157457.3526\text{K}$, $n_e = 1.61 \cdot 10^{24}\text{cm}^{-3}$, $\Gamma_{ee} = 2$. As the length scale we use the electron plasma frequency $\omega_p = n_e e^2 / \epsilon_0 m_e$.



a)



b)

Fig. 11. Comparisons among the normalized dynamic structure factors of Alkali plasmas (Na^+ , K^+ , Rb^+ , Cs^+) and results obtained by S. Adamjan et al. [53] at for Hydrogen-like plasma $k = 1.534 \cdot r_{ee}$, (a) $T = 1574573.526\text{K}$, $n_e = 2.5 \cdot 10^{25}\text{cm}^{-3}$, $\Gamma_{ee} = 0.5$ and (b) $T = 157457.3526\text{K}$, $n_e = 1.61 \cdot 10^{24}\text{cm}^{-3}$, $\Gamma_{ee} = 2$. As the length scale we use the electron plasma frequency $\omega_p = n_e e^2 / \epsilon_0 m_e$.

2. F. Hensel, S. Juengst, F. Noll, R. Winter, *In Localisation and Metal Insulator Transitions*, ed. D. Adler, H. Fritsche, (Plenum Press, New York, 1985).
3. W. Freyland, Phys. Rev. B **20**, 5140 (1979).
4. S. Juengst, B. Knuth, F. Hensel, Phys. Rev. Lett. **55**, 2160 (1985).
5. R. Winter, F. Hensel, et al., J. Phys. Chem. **92**, 7171-7174 (1988).

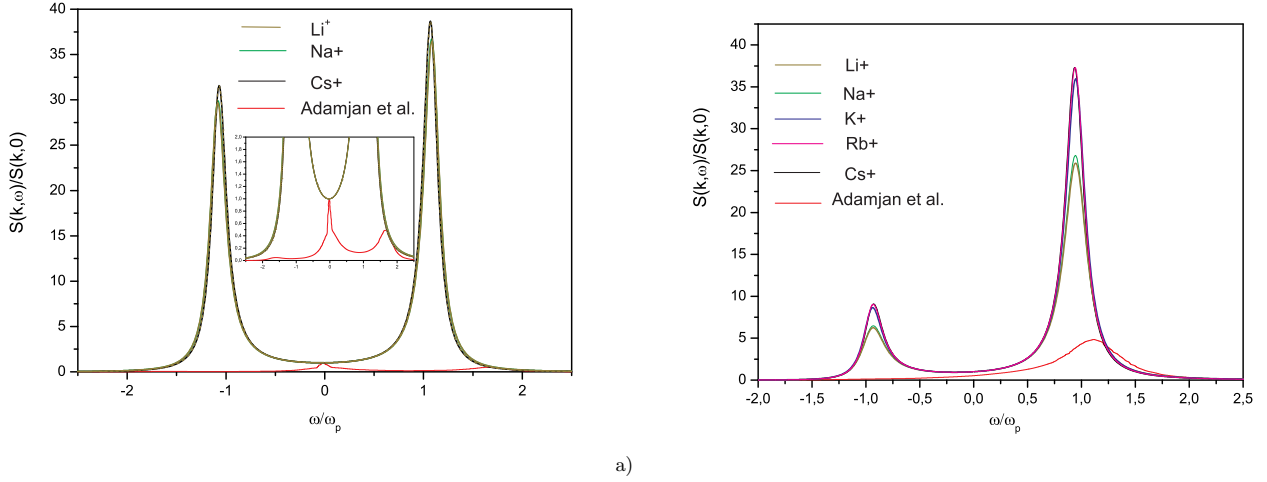


Fig. 12. Comparisons among the normalized dynamic structure factor of Alkali plasmas (a) (Li^+ , Na^+ , Cs^+) and (b) (Li^+ , Na^+ , K^+ , Rb^+ , Cs^+) and results obtained by S. Adamjan et al. [53] at $k = 0.767 \cdot r_{ee}$, (a) $T = 30000\text{K}$, $n_e = 1.741 \cdot 10^{20}\text{cm}^{-3}$, $\Gamma_{ee} = 0.5$ and (b) $T = 30000\text{K}$, $n_e = 1.11 \cdot 10^{22}\text{cm}^{-3}$, $\Gamma_{ee} = 2$. As the length scale we use the electron plasma frequency $\omega_p = n_e e^2 / \varepsilon_0 m_e$.

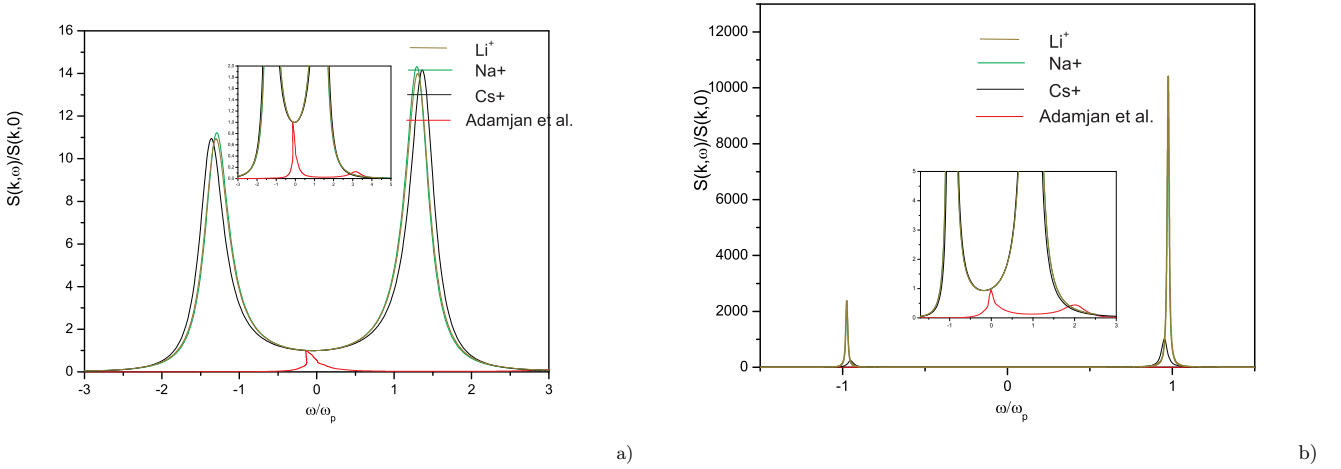


Fig. 13. Comparisons among the normalized dynamic structure factors of Alkali plasmas (Li^+ , Na^+ , Cs^+) and results obtained by S. Adamjan et al. [53] at for Hydrogen-like plasma $k = 1.534 \cdot r_{ee}$, (a) $T = 30000\text{K}$, $n_e = 1.741 \cdot 10^{20}$, $\Gamma_{ee} = 0.5$ and (b) $T = 30000\text{K}$, $n_e = 1.11 \cdot 10^{22}\text{cm}^{-3}$, $\Gamma_{ee} = 2$. As the length scale we use the electron plasma frequency $\omega_p = n_e e^2 / \varepsilon_0 m_e$.

6. N. F. Mott, *Metal-Insulator Transitions*, (Taylor and Francis, London, 1974).

8. W. Ebeling, A. Foerster, W. Richert, H. Hess, *Physics A* **150**, 159 (1988).

7. R. E. Goldstein, N. W. Aschcroft, *Phys Rev Lett.* **55**, 2164 (1985).

9. H. Hess, *Physics of nonideal plasmas*, eds. W. Ebeling, A. Foerster, R. Radtke, B. G. Teubner, (Leipzig, 1992).

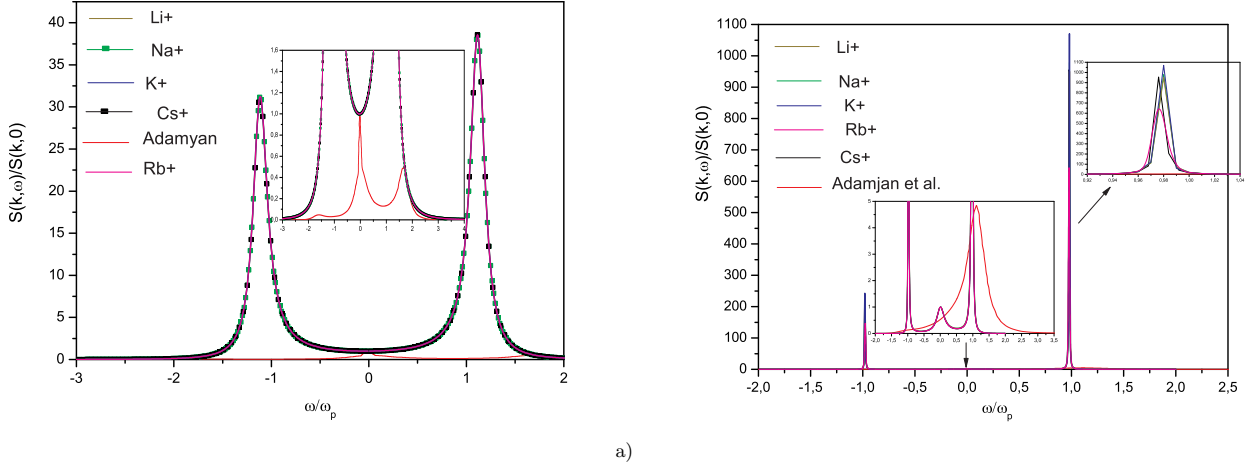


Fig. 14. Comparisons among the normalized dynamic structure factor of Alkali plasmas (Li^+ , Na^+ , K^+ , Rb^+ , Cs^+) with the modified H (36) and $L'(k)$ (37) and results obtained by S. Adamjan et al. [53] at $k = 0.767 \cdot r_{ee}$, (a) $T = 30000K$, $n_e = 1.741 \cdot 10^{20} \text{ cm}^{-3}$, $\Gamma_{ee} = 0.5$ and (b) $T = 30000K$, $n_e = 1.11 \cdot 10^{22} \text{ cm}^{-3}$, $\Gamma_{ee} = 2$. As the length scale we use the electron plasma frequency $\omega_p = n_e e^2 / \epsilon_0 m_e$.

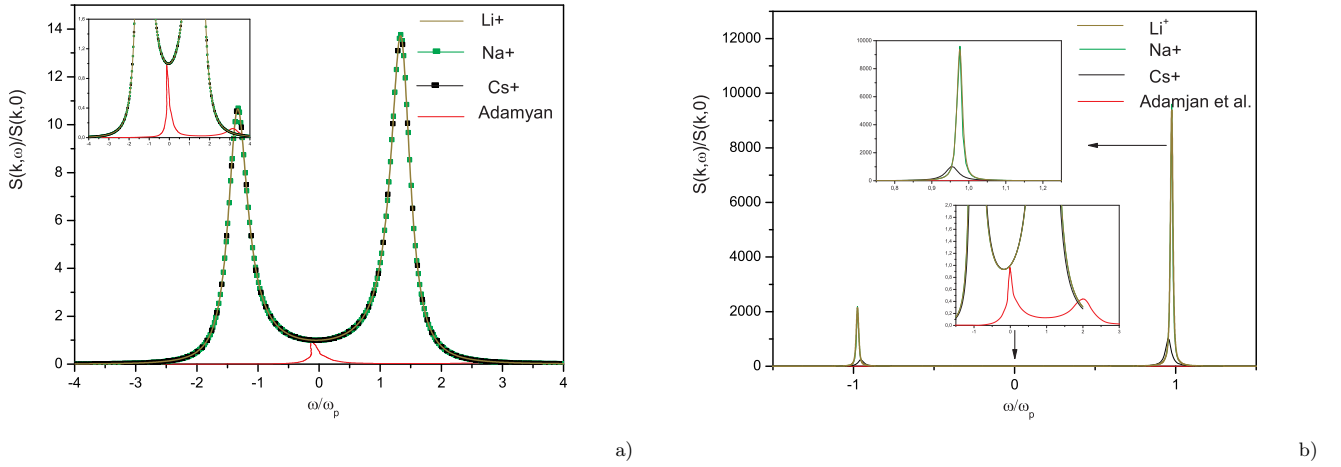
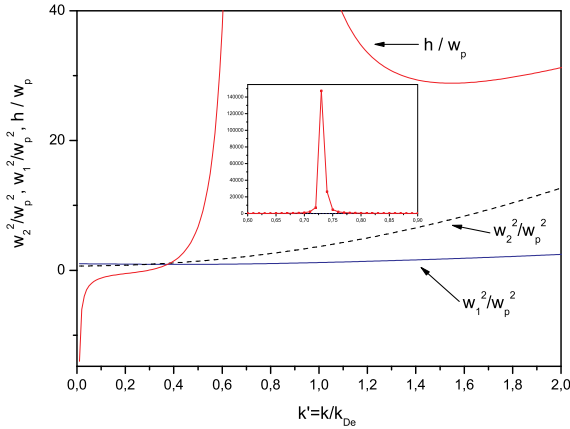


Fig. 15. Comparisons among the normalized dynamic structure factors of Alkali plasmas (Li^+ , Na^+ , Cs^+) with the modified H (36) and $L'(k)$ (37) and results obtained by S. Adamjan et al. [53] at for Hydrogen-like plasma $k = 1.534 \cdot r_{ee}$, (a) $T = 30000K$, $n_e = 1.741 \cdot 10^{20}$, $\Gamma_{ee} = 0.5$ and (b) $T = 30000K$, $n_e = 1.11 \cdot 10^{22} \text{ cm}^{-3}$, $\Gamma_{ee} = 2$. As the length scale we use the electron plasma frequency $\omega_p = n_e e^2 / \epsilon_0 m_e$.

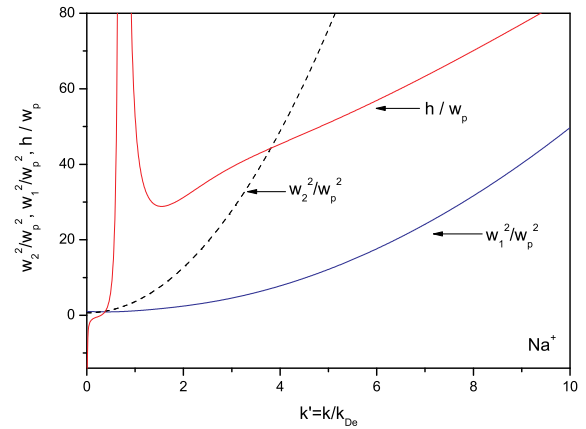
10. U. Seydel, W. Frucke, H. Wadle, *Die Bestimmung thermophysikalischer Daten flüssiger hochschmelzender Metalle mit schnellen Pulsaufheizexperimenten*, (Verlag Dr. P. Mannhold, Duesseldorf, 1980).

11. V. Sizyuk, A. Hassanein, and T. Sizyuk, J. Appl. Phys. **100**, 103106 (2006).

12. S. Lorenzen, A. Wierling, H. Reinholz, G. Roepke, Contr. Plasma Phys. **48**, 657 (2008)



a)



b)

Fig. 16. the h/w_p , w_1^2/w_p^2 , w_2^2/w_p^2 for Na^+ plasma with the modified H (36) and $L'(k)$ (37) at $T = 30000\text{K}$, $n_e = 1.11 \cdot 10^{22}\text{cm}^{-3}$, $\Gamma_{ee} = 2$, $r_s = 5.24$, $\omega_p = n_e e^2 / \epsilon_0 m_e$.

13. S. Sadykova, W. Ebeling, I. Valuev and I. Sokolov, *Contrib. Plasma Phys.* **49**, 76–89 (2009)
14. G. Gregori, O.L. Landen, S.H. Glenzer, *Phys. Rev. E* **74**, 026402 (2006).
15. G. Gregori, A. Ravasio, A. Höll, S. H. Glenzer, S. J. Rose, *High Energy Phys.* **3**, 99-108 (2007).
16. P. Seufferling, J. Vogel, and C. Toepffer, *Phys. Rev. A* **40**, 323(1989).
17. H. R. Griem, *Spectral Line Broadening by Plasmas*, (Academic Press, New York, 1974).
18. G. Ecker, *Z. Physik* **148**, 593 (1957); G. Ecker and K.G. Müller, *Z. Physik* **153**, 317 (1958).
19. M.-M. Gombert, *Phys. Rev. E* **66**, 066407 (2002).
20. V.M. Zamalin, G.E. Norman, V.S. Filinov, *The Monte-Carlo Method in Statistical Mechanics* (in Russ.), (Nauka, Moscow, 1977).
21. J. P. Hansen, and I.R. Mc. Donald, *Phys. Rev. A* **23**, 2041 (1981).
22. C. Pierleoni, D.M. Ceperley, B. Bernu and W.R. Magro, *Phys. Rev. Lett.* **73**, 2145 (1994).
23. D. Klakow, C. Toepffer and P.-G. Reinhard, *Phys. Lett. A* **192**, 55 (1994); *J. Chem. Phys.*, **101**, 10766 (1994).
24. J.I. Penman, J. Clerouin and P. G. Zerah, *Phys. Rev. E* **51**, R5224, (1995).
25. A.V. Filinov, M. Bonitz and W. Ebeling, *J. Phys. A.: Math. Gen.* **36**, 5957-5962 (2003).
26. H. Wagenknecht, W. Ebeling, A. Forster., *Contrib. Plasma Phys.* **41**, 15-25 (2001).
27. H. Hellmann, *J. Chem. Phys.* **3**, 61 (1935); *Acta Fizicochem. USSR* **1**, 913 (1935); *Acta Fizicochem. USSR* **4**, 225 (1936); H. Hellmann and W. Kassatotschkin, *Acta Fizicochem. USSR* **5**, 23 (1936).
28. J. V. Abarenkov, V. Heine, *Phil. Mag.*, **9**, 451 (1964).
29. W. A. Harrison, *Pseudopotentials in the Theory of Metals*, (Benjamin, New York, 1966).
30. V. Heine, Cohen M.H., Weaire D., *Pseudopotential theory*, (Mir, Moskva, 1973).
31. G. L. Krasko, Z. A. Gurskii, *JETP letters* **9**, 363 (1969).
32. Z. A. Gurski, G. L. Krasko, *Doklady Akademii Nauk SSSR* (in russ) **197**, 810 (1971).

33. W. Ebeling, W.-D. Kraeft, D. Kremp, *Theory of Bound State and Ionization Equilibrium in Plasmas and Solids*, (Akademie-Verlag, Berlin, 1976).
34. W. Zimdahl, W. Ebeling, Ann. Phys. (Leipzig) **34**,9 (1977); W. Ebeling, C.-V. Meister and R. Saendig, 13 ICPIG, (Berlin, 1977) 725.; W. Ebeling, C.V. Meister, R. Saendig, Ann. Phys. **36**, 321 (1979).
35. W. Ebeling, V. Meister, R. Saendig, W.D. Kraeft, Ann. Phys. **36**, 321, (1979).
36. N.N. Bogoljubow, *Problem of a dynamical theory in statistical physics*, (GITTL, Moscow, 1946); *Studies in Statistical Mechanics*, Engl. Transl., ed. J. De Boer, G.E. Uhlenbeck, (North-Holland, Amsterdam, 1962).
37. H. Falkenhagen, *Theorie der Elektrolyte*, (S. Hirzel Verlag, Leipzig, 1971), p. 369.
38. F.B. Baimbetov, Kh. T.Nurekenov, T. Ramazanov, Phys. Lett. A **202**, 211 (1995).
39. Yu. V. Arkhipov, F.B. Baimbetov, A.E. Davletov, Eur.Phys. J. D **8**, 299-304 (2000).
40. G. Kelbg, Ann. Physik **13** 354, **14** 394 (1964).
41. W. Ebeling, G.E. Norman, A.A. Valuev, and I. Valuev, Contrib. Plasma Phys. **39**, 61 (1999).
42. L. Szasz, *Pseudopotential Theory of Atoms and Molecules*, (Wiley-Intersc., New York, 1985).
43. W. H. E. Schwarz, Acta Phys. Hung., **27**, 391 (1969); Theor. Chim. Acta (Berl.), **11**, 307 (1968).
44. N.P. Kovalenko, Yu. P.Krasnyj, U. Krey, *Physics of Amorphous Metals*, (Wiley-VCH, Weinheim, 2001).
45. H. Ebert, *Physikalisches Taschenbuch*, (Vieweg & Sohn, Braunschweig, 1967).
46. C. Deutsch, Phys. Lett. A **60**, 317 (1977).
47. H. Minoo, M. M. Gombert, C. Deutsch, Phys. Rev. A **23**, 924 (1981).
48. J. Chihara, J. Phys. F: Met. Phys. **17**, 295 (1987); J. Phys.: Condens. Matter **12**, 231 (2000).
49. D. Riley, N.C. Woolsey, D. McSherry, I. Weaver, A. Djaoui, and E. Nardi, Phys. Rev. Lett. **84**, 1704 (2000).
50. L. Pauling and J. Sherman, Z. Kristallogr. **1**, 81 (1932).
51. J. P. Hansen, E. L. Pollock, I. R. McDonald, Phys. Rev. Lett. **32**, 277 (1974)
52. V. M. Adamyan, I. M. Tkachenko, Teplofiz. Vys. Temp. **21**,417 (1983)[High Temp. (USA) **21**, 307 (1983)]; V. M. Adamyan, T. Meyer and I. M. Tkachenko, Fiz. Plazmy **11**, 826 (1985) [Sov. J.Plasma Phys. **11**, 481 (1985)].
53. S. V. Adamjan, I. M. Tkachenko, et al., Phys. Rev. E **48**, 2067 (1993).
54. N. I. Akhieser, *The classical Moment Problem* (Oliver and Boyd, London, 1965).
55. Yu. V. Arkhipov, A. Askaruly, D. Ballester, A. E. Davletov, G. M. Meirkhanova, I. M. Tkachenko, Phys. Rev E **76**, 026403, (2007).
56. S. Ichimaru, *Statistical Plasma Physics*, Vol. I: Basic Principles, (Addison-Wesley, Redwood City, 1992).
57. C. Fiolhais, J. P. Perdew, S. Q. Armster, and J. M. MacLaren, Phys. Rev. B **51**, 14001 - 14011 (1995).
58. S.S. Dalgic, S. Dalgic, G. Tezgor, Phys. Chem. Liq. **40**(5), 539, (2002).
59. E. Apfelbaum, Phys. Chem. Liq., GPCH-2009-0045.